Supplementary Information

Phosphorene-Derived Ni_2P/NiO Lateral Heterostructure for Highly Sensitive and Selective H_2S Gas Detection

Shutong He,[a] Lei Li,[a] Yaoda Liu,[a] Jie Su,[a] Yudong Sun*[b] and Zhengfei Dai*[a]*

[a] State Key Laboratory of Porous Metal Materials, Xi'an Jiaotong University, Xi'an 710049, China; E-mail: sensdai@mail.xjtu.edu.cn (Z.D.); xjlilei@stu.xjtu.edu.cn (L.L).

[b] Department of Vascular Surgery, Department of General Surgery, Ruijin Hospital, Shanghai Jiao Tong University School of Medicine, Shanghai 200025, China; E-mail: sunyudong@smmu.edu.cn (Y. S.).

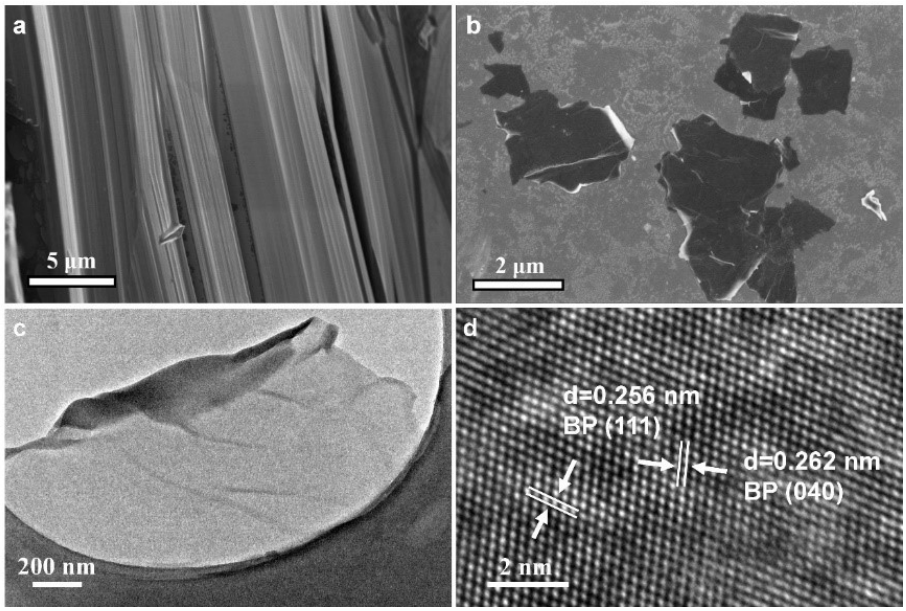

Fig. S1 (a) SEM image of BP bulk. (b) SEM image, (c) TEM image, and (d) HRTEM image of BP nanosheets.

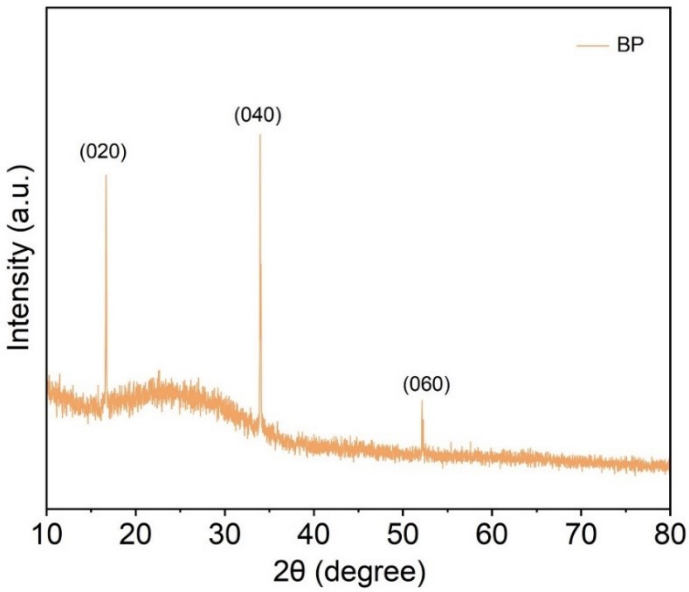

Fig. S2 XRD pattern of BP.

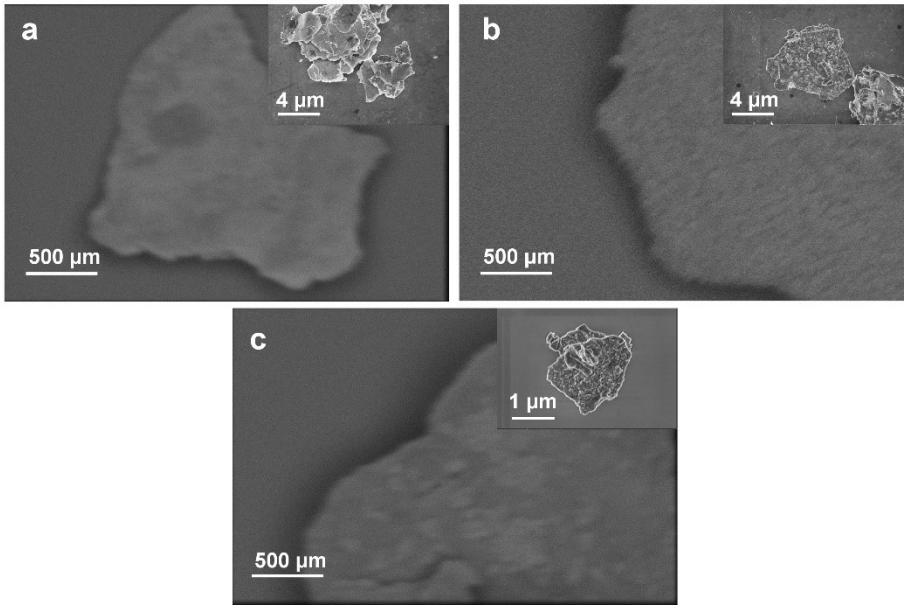

Fig. S3 SEM image of (a) $Ni_2P/Ni_{12}P_5$, (b) Ni_2P/NiO-4h, and (c) Ni_2P/NiO-16h.

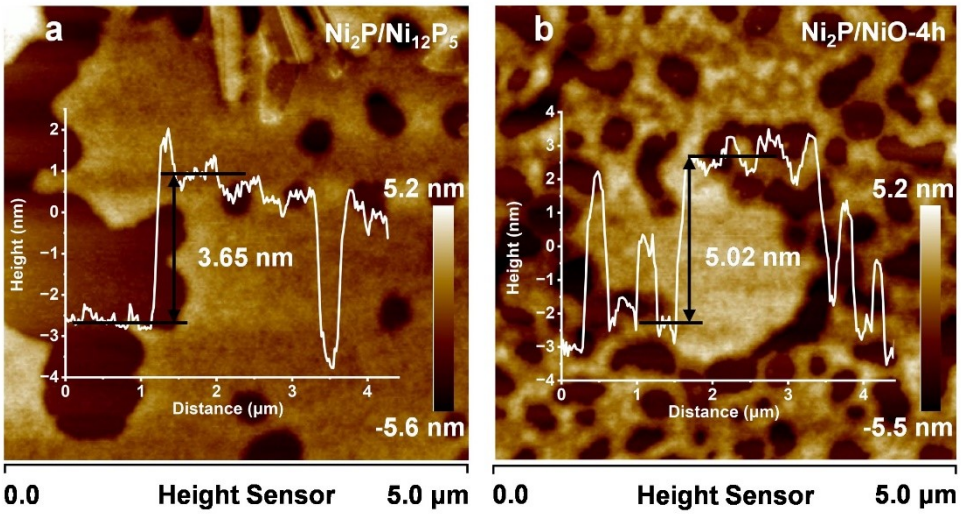

Fig. S4 AFM analysis of (a) $Ni_2P/Ni_{12}P_5$ and (b) Ni_2P/NiO-4h.

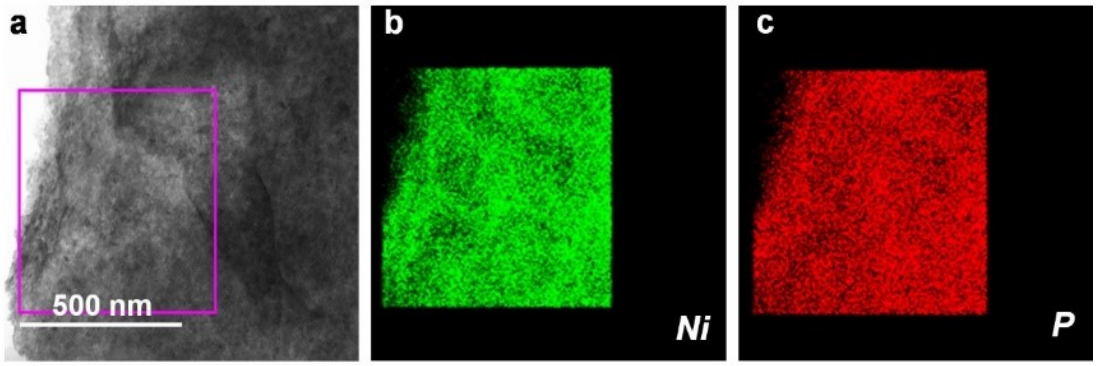

Fig. S5 (a) TEM image and (b-c) elemental mapping images of $Ni_2P/Ni_{12}P_5$.

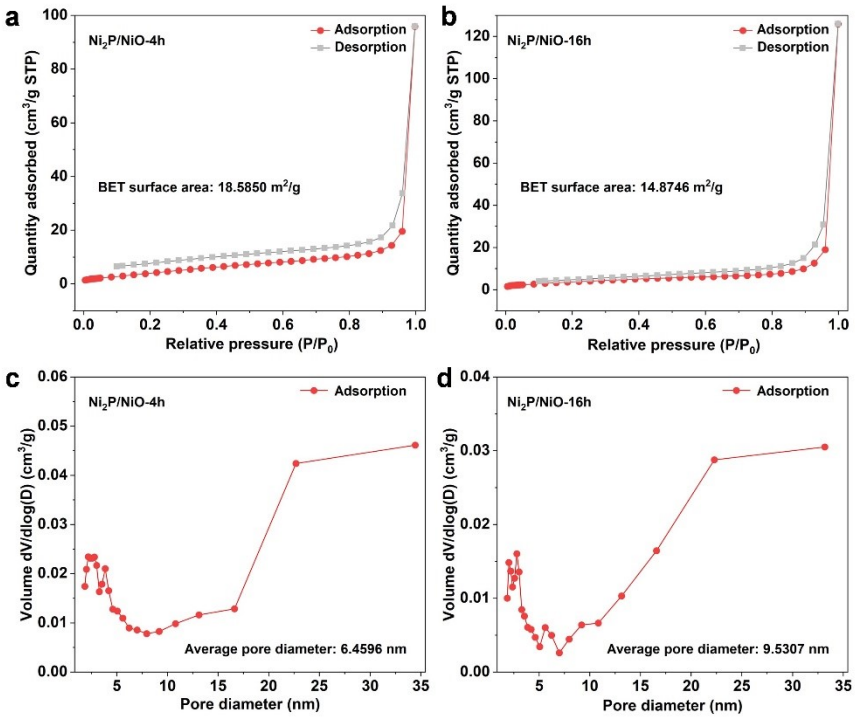

Fig. S6 (a) N_2 adsorption-desorption curve of the Ni_2P/NiO-4h and (b) Ni_2P/NiO-16h.

(c) The BJH pore size distribution of Ni_2P/NiO-4h and (d) Ni_2P/NiO-16h.

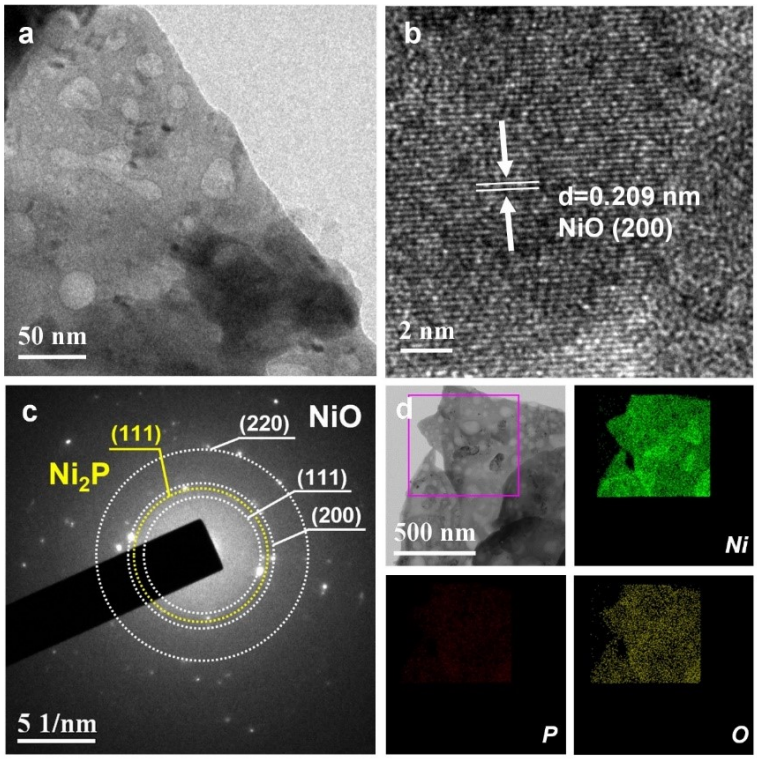

Fig. S7 (a) TEM image, (b) HRTEM image, (c) SAED pattern, and (d) elemental mapping images of Ni_2P/NiO-16h.

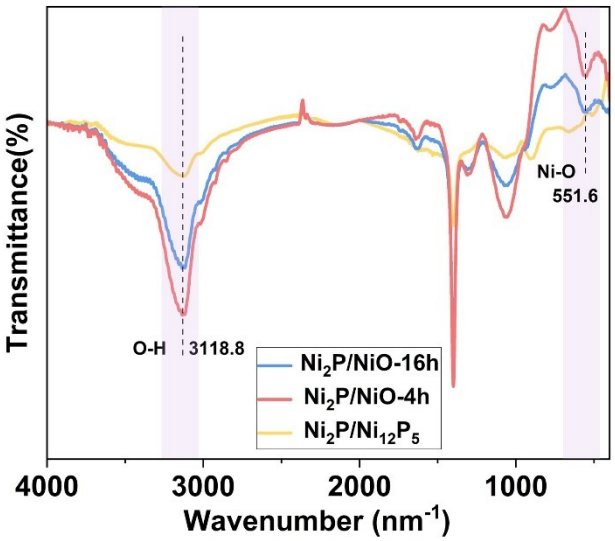

Fig. S8 FTIR spectra of $Ni_2P/Ni_{12}P_5$, Ni_2P/NiO-4h, and Ni_2P/NiO-16h.

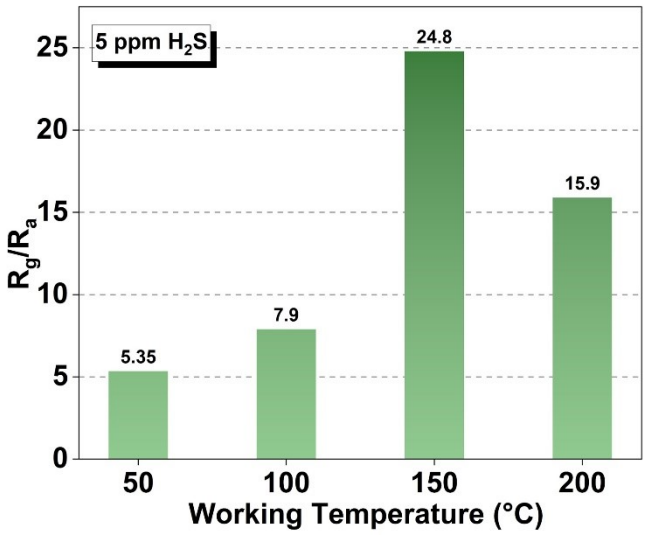

Fig. S9 Response values of Ni_2P/NiO-4h to 5 ppm H_2S at different temperatures.

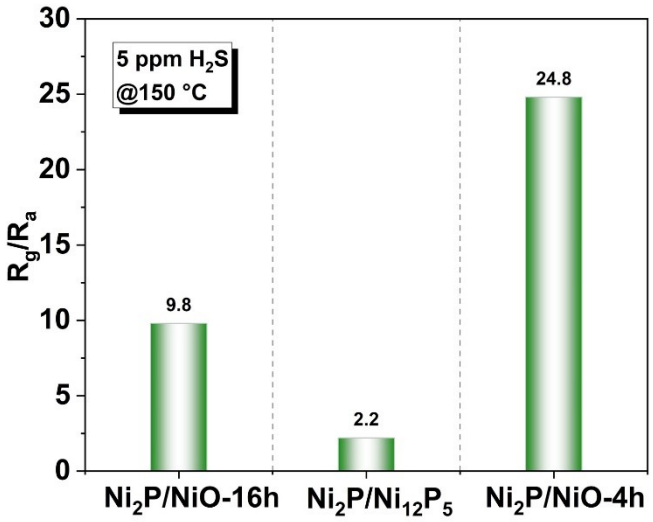

Fig. S10 Response values of $Ni_2P/Ni_{12}P_5$, Ni_2P/NiO-4h, and Ni_2P/NiO-16h to 5 ppm H_2S at 150 ℃.

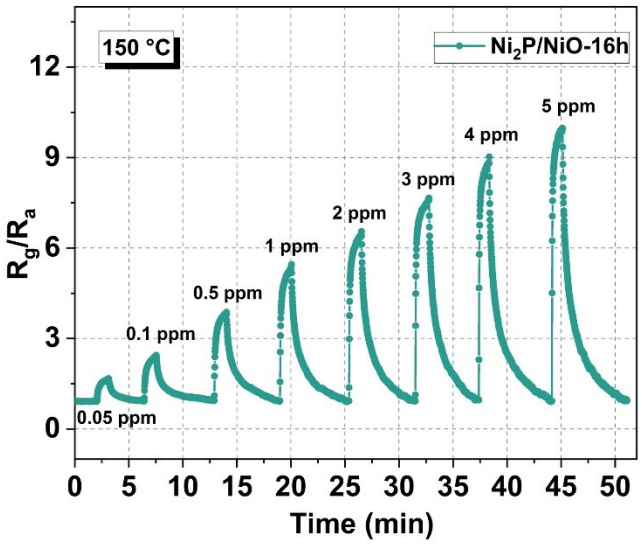

Fig. S11 Ni_2P/NiO-16h sensor response curve to 0.05-5 ppm H_2S at 150 ℃.

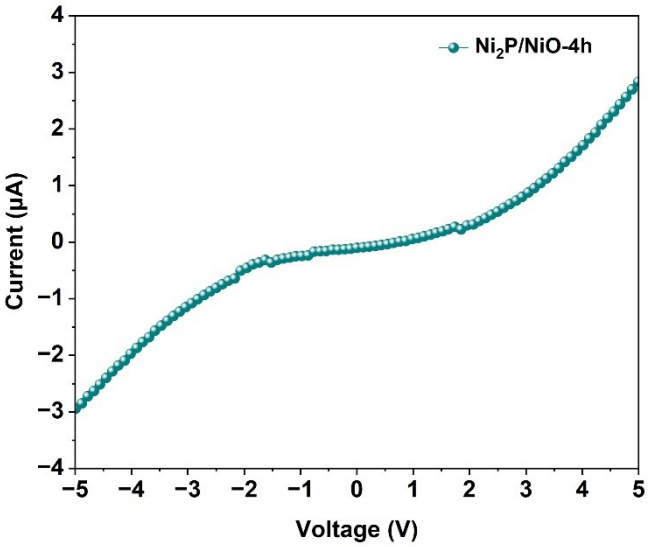

Fig. S12 I-V characteristics of Ni_2P/NiO-4h gas sensor.

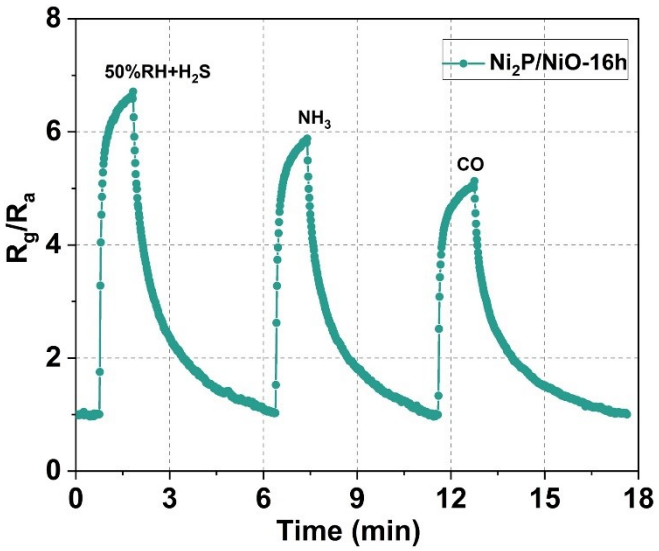

Fig. S13 Ni_2P/NiO-16h gas sensor responses to 50%RH+H_2S, NH_3, and CO.

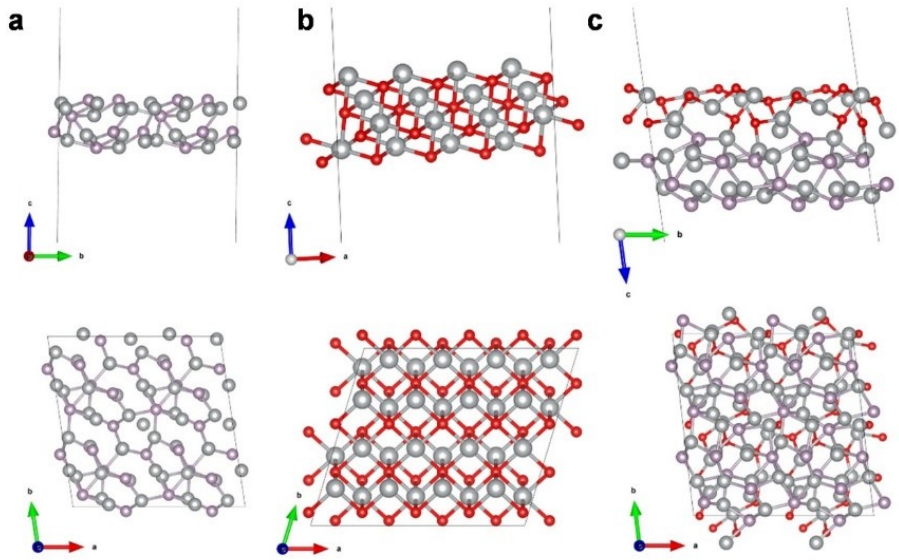

Fig. S14 Theoretical structural model of (a) Ni_2P, (b) NiO, and (c) Ni_2P/NiO heterostructure (Atoms are colored as follows: Ni, gray; P, purple; O, red).

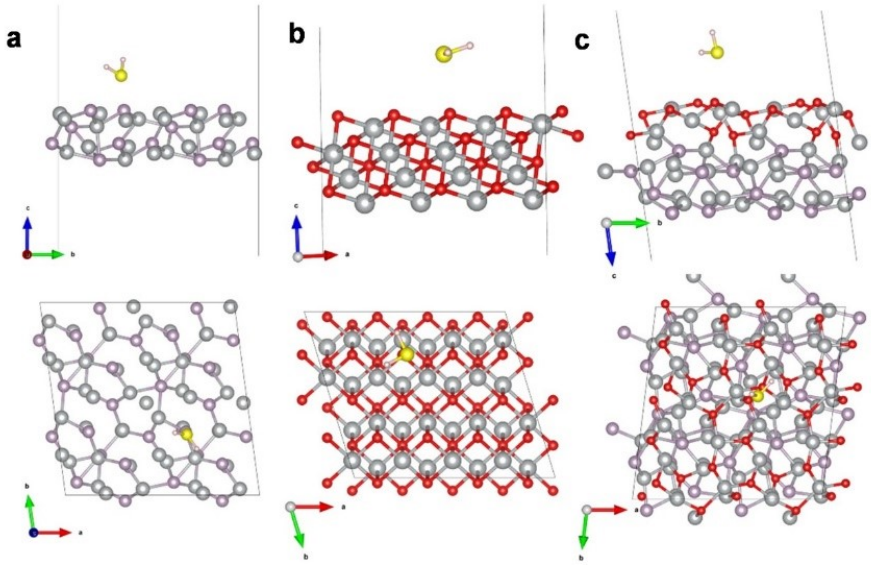

Fig. S15 Theoretical structural model for H_2S molecular adsorption of (a) Ni_2P, (b) NiO, and (c) Ni_2P/NiO heterostructure (Atoms are colored as follows: Ni, gray; P, purple; O, red; S, yellow; H, pink).

Table. S1 The quantitative composition of Ni, P, and O in the samples by ICP analysis (wt %).

Sample	Ni	P	O
$Ni_2P/Ni_{12}P_5$	74.25	23.32	2.43
Ni_2P/NiO-4h	67.85	13.39	18.76
Ni_2P/NiO-16h	65.63	5.81	28.56

The mass fraction of P in Ni_2P is 20.87%, and the P element only exists in the Ni_2P part in the Ni_2P/NiO-4h composite. According to the ICP results, the P weight ratio in the Ni_2P/NiO-4h is 13.39%. So, the Ni_2P weight ratio in the Ni_2P/NiO-4h can be calculated as 13.39%/20.87%=64.18%, and thus the NiO weight ratio is 35.82 wt%.

Table. S2 Comparison of sensing performance based on NiO materials towards H_2S in the previous literatures.

Sensing materials	Working Temperature	Gas concentration	Response (R_g/R_a)	Detection limit	Ref.
ZnO-NiO	250 ℃	5 ppm	1.5	1 ppm	[1]
Zn/NiO	270 ℃	2 ppm	3.23	0.05 ppm	[2]
Co-NiO@g-C_3N_4-3	172 ℃	20 ppm	45	5 ppm	[3]
α-Fe_2O_3/NiO	300 ℃	20 ppm	239	0.25 ppm	[4]
NiO epitaxial films	300 ℃	100 ppm	13.07	0.186 ppm	[5]
$NiWO_4$(5%)-NiO	20 ℃	1 ppm	7.36	0.1 ppm	[6]
Fe-NiO_x	270 ℃	0.8 ppm	5.24	0.05 ppm	[7]
NiO thin films	350 ℃	100 ppm	14.8	3 ppm	[8]
Ni_2P/NiO-4h	**150 ℃**	**5 ppm**	**24.8**	**0.05 ppm**	**This work**

Reference

1. J. N. O. Amu Darko, S. Hussain, E. Issaka, M. Wang, A. A. Alothman, S. Lei, G. Qiao and G. Liu, *Ceram. Int.*, 2024, **50**, 17681–17690.
2. O. Wang, J. W. Kong, Z. G. Xue, B. L. An, J. Q. Xu and X. H. Wang, *ACS Sensors*, 2024, **9**, 3233–3243.
3. W. J. Du, X. Y. Su, H. Yang, S. H. Dong, L. Chen, J. F. Shang, L. X. Su, S. H. Liu, L. L. Wu and N. N. Wu, *Ceram. Int.*, 2024, **50**, 47939–47948.
4. N. D. Cuong, V. H. Sinh, D. T. Quang, L. T. Hoa, V. V. Tan, H. D. Mai, K. J. Jeon, P. H. Phuoc and N. V. Hieu, *Curr. Appl Phys.*, 2024, **59**, 153–164.
5. L. L. Kuang, T. Xiang, J. X. Li, S. Y. Wu, Y. Q. Dong, Q. Y. He, J. W. Xue, X. Y. Chen, Y. J. Tao, Y. T. Wang, H. Jin, J. X. Yi and Z. L. Luo, *Chin. J. Chem. Phys.*, 2025, **38**, 272–280.
6. J. S. Guo, D. Z. Zhang, J. D. Bian, J. S. Zhai, P. L. Jia and X. Y. Ji, *IEEE Sens. J.*, 2025, **25**, 117–124.
7. Y. Chen, T. W. Yuan, Y. X. Li, B. Shen, W. S. Zhang, J. Q. Xu and M. H. Wu, *Ceram. Int.*, 2024, **50**, 22243–22251.
8. S. Srivastava, A. K. Gangwar, A. Kumar, G. Gupta and P. Singh, *Micro Nanostruct.*, 2023, **184**, 207678.